NISTIR 6030

THIRTEENTH MEETING OF THE UJNR PANEL ON FIRE RESEARCH AND SAFETY, MARCH 13-20, 1996

VOLUME 1

Kellie Ann Beall, Editor

June 1997
Building and Fire Research Laboratory
National Institute of Standards and Technology
Gaithersburg, MD 20899

U.S. Department of Commerce
William M. Daley, *Secretary*
Technology Administration
Gary R. Bachula, *Acting Under Secretary for Technology*
National Institute of Standards and Technology
Robert E. Hebner, *Acting Director*

RADIATION TRANSFER AND TEMPERATURE DISTRIBUTION IN A FEW SMALL POOL FLAMES

HIROSHI HAYASAKA
Faculty of Engineering
Hokkaido University
Sapporo, 060, JAPAN

ABSTRACT

A new way of using thermography for radiative objects like pool flames is introduced and applied to small pool flames. Radiative characteristics and flame structure of small pool flames are considered by examining flame temperature distribution from a radiation point of view. In addition, it is shown that pool flame structure for various fuels becomes more clear when the standard deviation and the coefficient of variation obtained from thermographic data are used.

INTRODUCTION

In fire fighting and fire safety science, the estimation of thermal radiation from tank fires to the surroundings is important. Many experimental and theoretical studies have been performed on this. Recently a new technique has been developed and used in fire experiments: Brötz et al. [1] have developed the equidensitometry technique based on the sensitometric wedge method. By processing a photographic negative using electronic equidensitometry, they determine lifetimes and migration velocities of eddies, etc. in pool flames. This technique is very effective in obtaining both instantaneous and mean characteristics of flames but there are difficulties with extracting statistical data such as standard deviation and coefficient of variation of radiance which would help establish the flame structure of pool flames.

Little is known of the effect of the combined radiation and combustion phenomena in pool flames. In a pool flame, radiation may control the burning rate and affect the combustion conditions in the flame. More information on radiation in pool flames may lead to the development of better ways to control this kind of fire. From this point of view, conversion from temperature to irradiance may be useful and meaningful. To address this, an alternative use of thermography has been developed by the authors [2,3]. Here, commercial thermography is used to obtain the irradiance distribution rather than the temperature distribution in pool flames of various fuels.

Experiments were conducted to determine the radiation characteristics of pool fires. The apparent temperature data obtained by thermography were converted to irradiance and radiance by simple calculations. Finally, statistical analysis related to radiance data was made to obtain the mean radiance and flame structure of the pool fire flames of three different fuels.

EXPERIMENT

Pool fire tests were carried out in a quiescent atmosphere. The experimental setup is shown in Fig. 1. A small stainless steel tank of diameter 48.5 mm and depth 14.5 mm was used for the pool fire tests. The burning rate was measured by an electric balance. Heptane, kerosene, and methanol were used as test fuels. Each fuel was fed into the tank by gravitational force and freeboard was kept almost zero (about 1 mm) by using a valve in the fuel line. The flame temperature distributions were measured by conventional chromel-alumel thermocouples of 0.3 mm diameter.

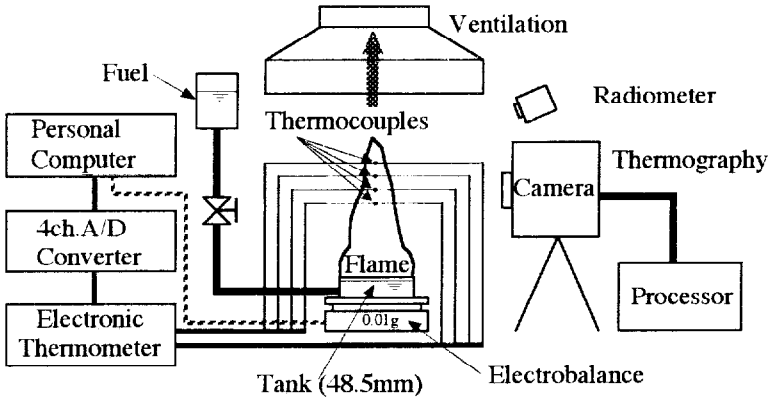

Figure 1. Schematic experimental arrangement for small pool flames.

The apparent temperature distribution of the pool flame was obtained with color television thermography which stored whole images of the pool flame on a floppy disk at a maximum speed of 20 frames/sec.. The thermographic equipment was installed at 25.4D (D is a the tank diameter, 0.0485 m in this paper). The thermography stored one thermal image as a TV color image with 25,600 data points. The apparent temperature distributions were converted to radiance distributions and irradiance using simple calculations. A series of 40 images were recorded continuously at 10 second intervals and were analyzed statistically to obtain not only the distribution of mean radiance but also standard deviation and coefficient of variation.

The irradiance of the pool flames was also measured with a conventional thermopile type radiometer having wide view angle and flat spectral range installed at 7 D. The radiometer and thermography data were compared to verify the validity of the thermographic data.

THERMOGRAPHY

The thermography used in the experiment has the spectral range from 3 to 5.4 microns. The display levels can be set to 256 colors. The high response InSb detector is cooled by argon gas, and provides whole pool flame images instantaneously. The data of the images can be stored at 0.05 second intervals or slower (0.5, 1 or several seconds). The digital data is recorded in a way that allows it to be reused and converted to physical quantities like temperature, irradiance, etc..

A thermograph is a radiation thermometer. The detector is a radiometer, and the output is interpreted in terms of temperature, considering the distance to the object, emissivity, and the area of the object, defined by the field of view or the thermographic device. This conversion is simple and reliable when the object is a solid with known emissivity and area. The distance to the object, emissivity, and area of object cannot easily be defined when the object is gaseous as with pool flames. As a result, direct thermographic images cannot be used as they indicate incorrect or apparent temperature distributions.

In this paper, an imaginary black body wall is introduced in front of pool flame and conversion of the apparent temperature distribution into radiance distribution is made to determine the thermal structure of the large scale pool flames. It is assumed that the imaginary wall is at the edge of the tank [2,3]. A data point, s, does not always represent the radiance of a pool flame just behind the imaginary wall. However, when the distance L is relatively large, as in this experiment, we may assume that the measured, apparent temperature distribution at the center of a thermographic image will not contain large locational errors.

The apparent temperature distribution can be converted to a radiance distribution by the calculations below. Thermography converts radiation heat to apparent temperature, T_a (K), with Equation (1):

$$T_a=(q_s(i,j)/(\varepsilon_s \sigma a_t))^{0.25}-T_\infty^{0.25} \quad (1)$$

where $q_s(i,j)$ is the radiance of data point s on the imaginary wall (kW/m^2), i,j are indices of the horizontal (x-axis) and vertical (z-axis) location and take values of 1 to 100 and 1 to 256 respectively, ε_s is the emissivity of data point s (=1), σ is the Stefan-Boltzmann constant (5.67×10^{-8} W/m^2/K^4); a_t is the area of a data point (m^2) obtained by the equation: $a_t=(2.17375 \times L+0.3456) \times 10^{-6}$ for the TVS-2000 used. Here L is the measured distance between thermography and imaginary wall (m), T_∞ is the background temperature. The constants in this equation are coefficients in a simple equation related to the view angle of the thermography.

Thus the radiance at s can be determined with $q_s(i,j)= \sigma a_t (T_a^4 - T_\infty^4)$ derived from Equation (1). The total radiant heat from an imaginary wall can be obtained with Equation (2).

$$Q_s=\sum_{i=1}^{m}\sum_{j=1}^{n} q_s(i,j) \quad (2)$$

where m=100 and n=256. Finally, Q_s, which is the irradiance observed at the distance L, is rescaled to the dimensionless distance L/D=5 to compare it with the data of the wide angle radiometer. It has units kW/m^2; $q_s(i,j)$ is simply divided by a solid angle(π) for a hemisphere on one side of the imaginary wall to convert it to radiance. This is the radiative heat emitted from the flame surface within a unit area to the surroundings per unit solid angle. Finally, $q_s(i,j)$ has the units kW/m^2/sr.

Forty continuous thermographic images were stored and processed by a personal computer to obtain the distribution of mean radiance, standard deviation and coefficient of variation. In this process, a 2x2 matrix of sixteen contiguous data points were integrated into one new data point. Thus, 25,600 (=100x256) data points were reduced to 6,400 (=50x128) to provide a smoother contour. $q_{s,k}(i',j')$ was introduced to represent the radiance of each new data point. The suffix k is the thermographic image number 1 to 40, i',j' indicate the location of a thermographic image and take values of 1 to 50 and 1 to 128 respectively.

RESULTS AND DISCUSSION

Previous Study of Flame Structure of a Pool Flame

Thomas [4] and McCaffrey [5], who studied the flame structure of buoyant diffusion flames similar to pool flames, plotted temperature rise from room temperature on the center line of the flame and defined three regions in the flame, namely the continuous flame region, the intermittent flame region and the plume region. The abscissa of their figure is $z/Q_c^{2/5}$ where z is the vertical height from the tank top, Qc is the nominal rate of heat release by combustion (kW). According to McCaffrey [5], who measured natural gas diffusion flames, the boundary between the regions are at abscissa values of 0.08 and 0.2. These values may be correct only for a flame from a low sooting, gaseous fuel. Boundary values for liquid fuels depend on the fuel properties because they need evaporation and decomposition regions in the bottom of flames or near the fuel surface. In addition, many hydrocarbon liquid fuels tend to produce soot. These characteristics may make a difference especially when the size of the pool flame is small. Thus fuel properties and flame dimensions may effect the measured temperature profiles. In any event, the region boundary values are a little bit different from the McCaffrey's values.

Irradiance of Three Different Fuels

The irradiances of the three fuels are shown in Fig. 2. The abscissa is the picture number; the 40 pictures are taken at 10 second intervals under steady state conditions. Measured mean burning rates of heptane, kerosene and methanol are 2.22, 1.47 and 2.0 (x10^{-2} kg/s/m^2)

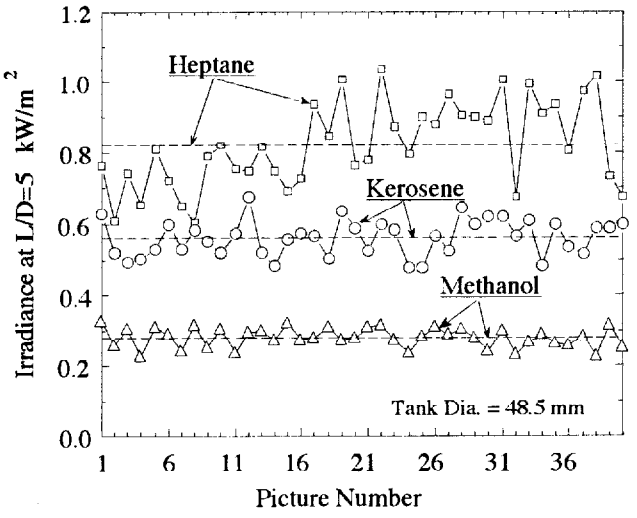

Figure 2. Irradiance of three fuels.

respectively. The ordinate of Fig. 2 is the irradiance at the dimensionless distance L/D=5. The irradiances of heptane, kerosene and methanol are shown by squares, circles and triangles respectively. Three dashed horizontal lines show the mean values of the forty data sets for the three fuels. The irradiance values for each fuel are almost the same as those obtained by the conventional wide angle radiometer. Fig. 2 shows that the mean irradiance of heptane is the highest and that of methanol is the lowest. Each symbol in Fig. 2 is the result of a thermographic image containing 25,600 data points.

Radiative Characteristics and Flame Structure

Contours of temperature, mean radiance, standard deviation and coefficient of variation for heptane, kerosene and methanol flames are shown in Figs. 3, 4, 5 and 6 respectively. Horizontal and straight dotted lines of each Fig. show the boundary of the continuous flame region, intermittent flame region and plume region. These boundary lines are drawn using experimental results. The z axis is defined as a vertical line perpendicular to the tank. The left side ordinate of each Fig. is the dimensionless height from the tank top, z/D. A theoretical expression to characterize buoyant diffusion flames proposed by Thomas and McCaffrey, $z/Q_c^{2/5}$, is used in the right side ordinate of each Fig..

Contours of temperature. The contours of temperature in Fig. 3 show that the heptane flame has the highest flame temperature of the three fuels, 1224 K. It also has the largest area of high temperature, indicated on the figure by dot-shading where the temperature exceeds 1000 K. By comparison, the highest flame temperature of kerosene is only 1085 K and the high temperature area, near the bottom of flame, is the smallest. The methanol flame's highest temperature is 1152 K. Its high temperature area is bigger than that of the kerosene flame.

The trace of local maximum temperature versus height is indicated by lines of heavy dots. These lines intersect on the flame axis near $z/Q_c^{2/5} = 0.8$. Inside these lines is relatively cool fuel, outside is air approaching the reaction zone. Along the line is a band of strong mixing where the combustion occurs. According to Bouhafid et al. [6], these bands coincide approximately with the location of the luminous flame envelope, particularly at the flame base.

Only for the methanol flame dose the line approximately coincide with the location of the top of the continuous flame region. Perhaps this is because methanol is sootless, yielding a blue flame. The sooty flames of heptane and kerosene are apparently different except near the base of the flame. Heptane and kerosene flames change their shape from a cone to a mushroom cap periodically. According to the recent report by Ito, et al.[7], this flame shape change cycles at

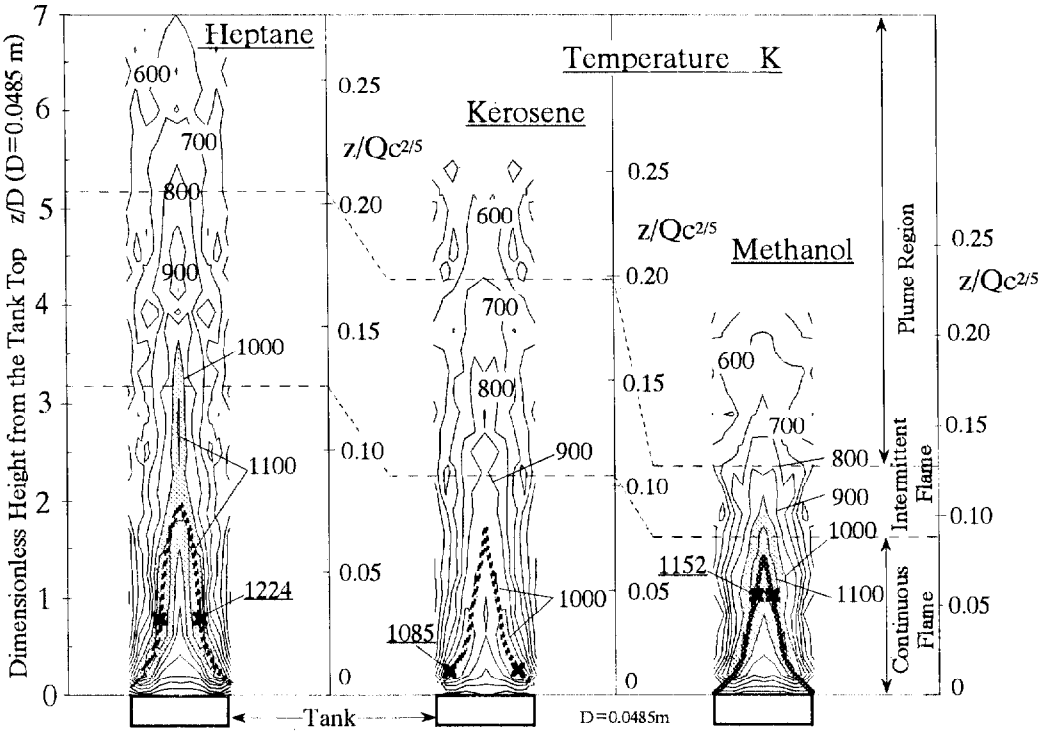

Figure 3. Temperature contours of three flames.

about 10 Hz for the size pool used here. Ito, et al. measured heptane pool flames using a high speed video camera. As a result of measurement, they showed the transition from a conical to a mushroom cap flame. Due to this flame shape change, the boundary of the flame in the middle part of flame could not be defined well using only temperature data measured by thermocouples.

We could not explain the irradiance differences among the three fuels in Fig. 2 using only the contours of temperature in Fig. 3. One should be carefully in interpreting the various contours obtained by thermography data analysis.

Contour of mean radiance. The contours of mean radiance of three fuels are shown in Fig. 4. The two dashed lines drawn in these figures are maximum radiance band. In each flame, a band of high radiance is located just inside the lines of the maximum local temperature shown in Fig. 3. In addition, for kerosene and heptane, there is a second band of high radiance above and detached from the lower one. The kerosene flame has the highest radiance value among the three fuels, 4.54 kW/m^2/sr. Nevertheless its flame temperature is the lowest. This discrepancy between radiance and temperature may be due to the difference of local soot, CO_2 and H_2O concentration of the three flames.

The non-luminous flame of methanol has its highest radiance region just above the tank or the fuel surface. This means the concentration of CO_2, H_2O and the temperature are relatively high compared with other regions. The less luminous upper part of this buoyant flame is diluted considerably by the surrounding air.

On the contrary, the luminous pool flames of kerosene and heptane have two high radiance zones: in the bottom of flame and in the upper part of continuous flame region. One is located at the bottom to middle of the continuous flame region and the other is located at the boundary of the continuous and intermittent flame region.

We may conclude that the high radiance zone in the flame bottom exists in common. This high radiance zone in the flame bottom supplies enough heat both to the fuel surface and to the upper part of flame to sustain pool burning. Thus, a so-called persistent or anchored flame is

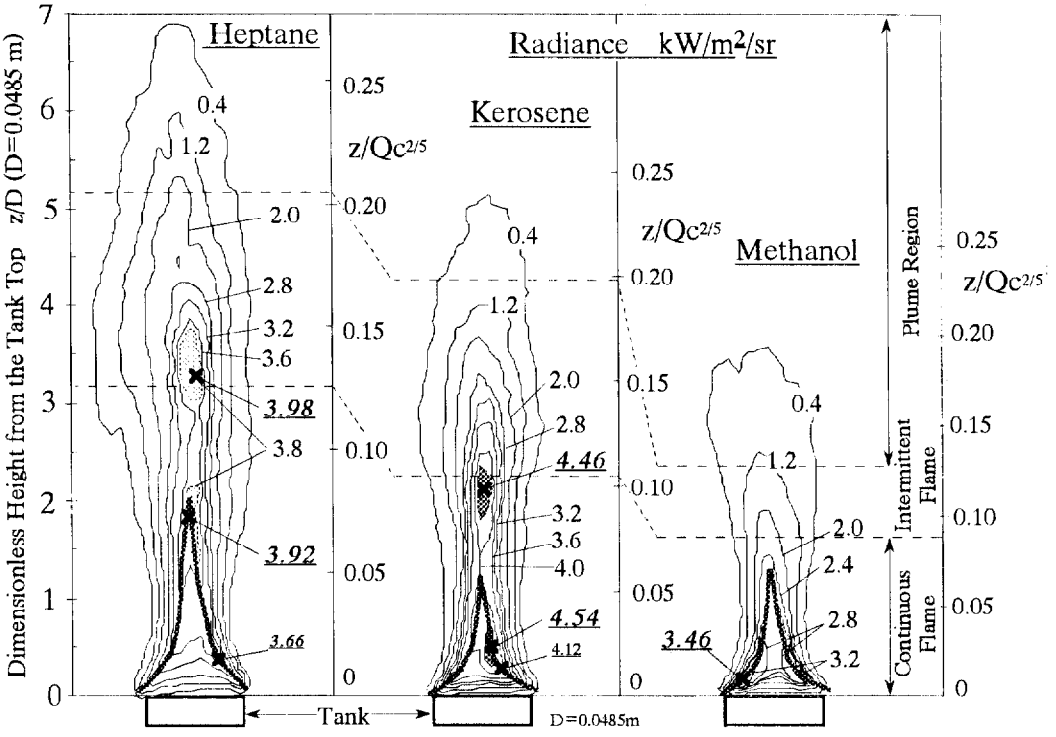

Figure 4. Radiance contours of three flames.

formed in the continuous flame region. The other high radiance zones in the middle of flame do not exist in the methanol flame. We may guess that this high radiance zone is related to soot. Pool flames seem to change their shape from a simple cone to a mushroom with cap periodically [7]. The top of the cone and the bottom of the mushroom cap are always formed near the upper part of continuous flame region or lower part of intermittent flame region. In other words, considerable unburned soot and gaseous fuel reaches the middle of flame and burns there. This area coincides to the above mentioned high radiance zones of kerosene and heptane.

Thus, the thermography technique has allowed us to identify one distinct radiative characteristics of the flame structure of small pool flames. This region was not detected well by the thermocouples because the flame moves upward with rapid radial expansion. This radial movement produces various size mushroom caps periodically. Temperature measurement by the thermocouples is less revealing in this region.

Contour of standard deviation. The contours of standard deviation in Fig. 5 indicate that all the flames have bigger values at the edge than in the center. Where the standard deviation is large, both the mean value and fluctuation are relatively large. This fluctuating flame region is where, alternately, relatively strong and week combustion reaction occur.

The highest values of the standard deviation are connected by a dashed line in Fig. 5. In relatively large pool flames, the dashed lines are considered to represent the average vortex paths where vortices were formed, grow, and dissipate. In small pool flames, as the vortex is not so large or the flame is laminar, the dashed lines almost coincide with the flame edge of each fuel within the continuous flame region. The high standard deviation region (exceeding 0.8) is observed in the intermittent flame region for each fuel. Especially, the high standard deviation region of heptane and kerosene is located just outside of the upper high radiance zones. The shape of the high standard deviation region may be considered like a ring or annulus. This means the mixing of air and fuel in this region is stronger than in other regions and a relatively large eddy forms here. As a result, the mushroom cap is produced near here; experimental

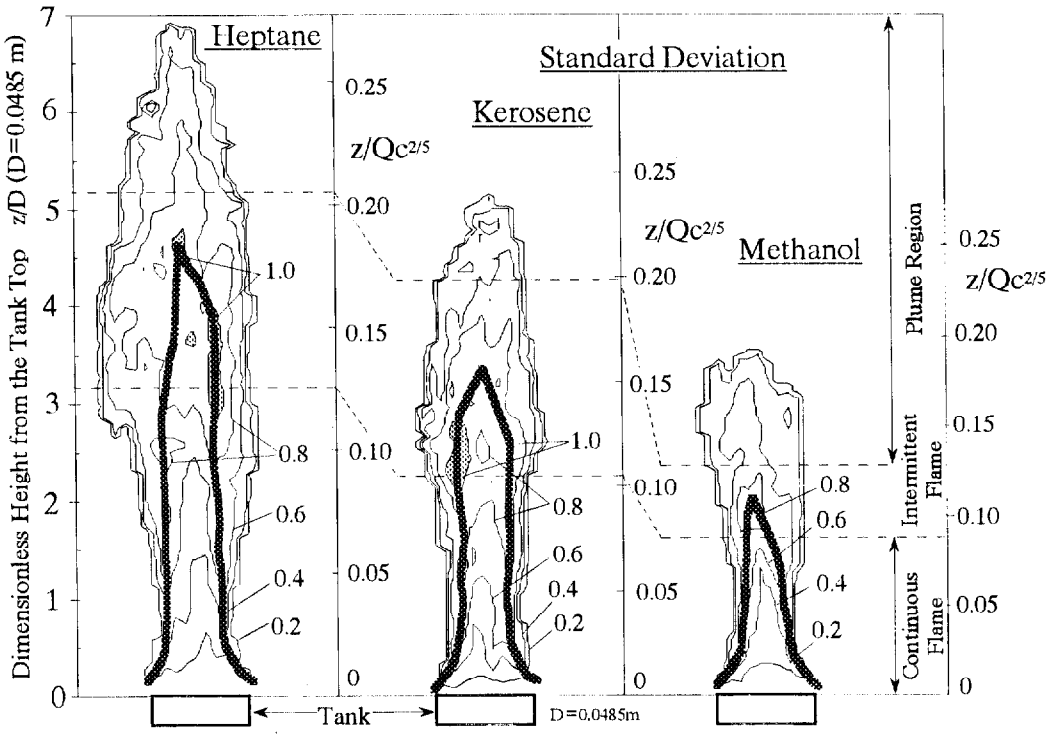

Figure 5. Standard deviation contours of three flames.

results support this idea [7].

Contour of coefficient of variation. Contours of coefficient of variation are shown in Fig. 6. The coefficient of variation expresses the magnitude of relative fluctuations irrespective of the magnitude of the mean radiance value because the coefficient of variation is obtained by dividing the standard deviation by the mean value. The coefficient of variation allows us to identify the stable region of the flame and the vortex formation and dissipation region.

Every flame has a region where the coefficient of variation is below 20%. This is at the base of the flame. Nevertheless there is great locational change of radiance due to active reaction between fuel and air. These stable regions play an important thermal role in pool flames, as described above.

The values of the coefficient of variation, on the flame center line, between the continuous and intermittent flame regions are about 50 % for heptane and kerosene, 70 % for methanol. The boundary values at the flame center between the intermittent and plume region are at 80 % for heptane, 120% for kerosene and 100 % for methanol. These differences may be because the methanol flame is sootless and the mushrooms cap flames are not made in the intermittent region.

Unfortunately, the large vortex formation and dissipation region is not observed in Fig. 6 because small pool flames are laminar. Only small size vortex regions are found at the bottom flame edge.

CONCLUSIONS

A new way of using thermography for radiative objects like pool flames is introduced and applied to small pool flames of three different fuels. Radiative characteristics and flame structure of small pool flames are considered by examining flame temperature distribution from a radiation point of view. In addition, it was shown that pool flame structure of various fuels became more clear when the standard deviation and the coefficient of variation obtained from

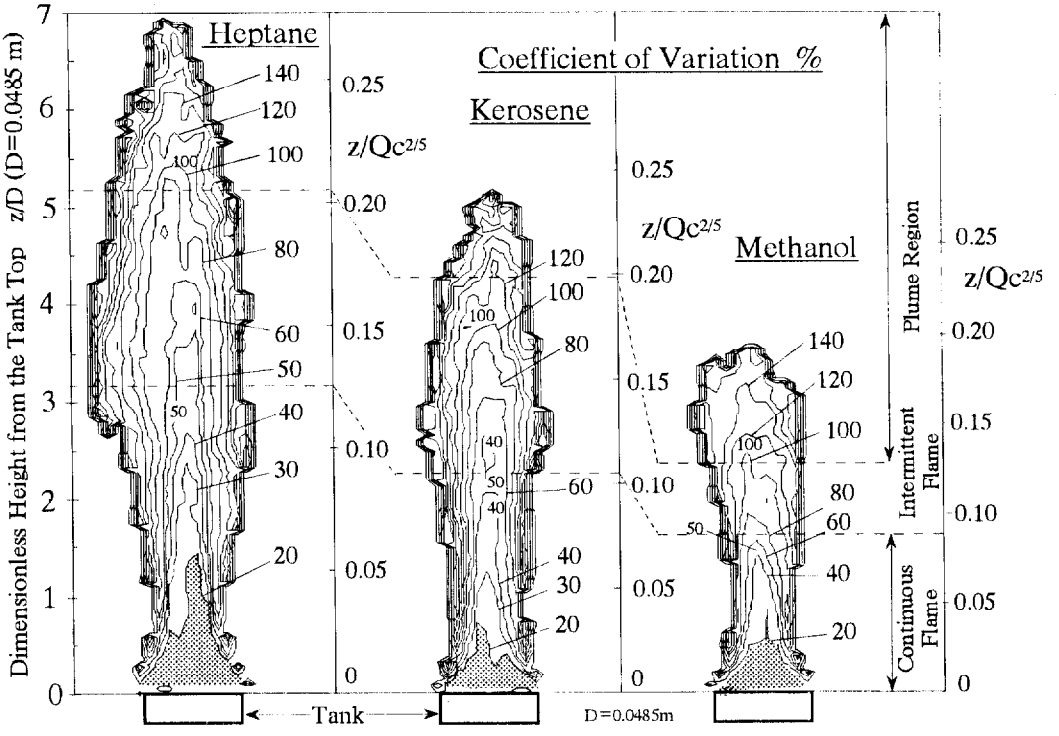

Figure 6. Contours of coefficient of variation of three flames.

thermographic data were used. The discussion allows the following conclusions:

(1) Small pool flames tend to have a high radiance zone in the continuous flame region. This high radiance zone is important to sustain pool flames thermally.

(2) In addition to the high radiance zone of the continuous flame region, luminous flames of heptane and kerosene have an upper high radiance zone near the boundary of the continuous and intermittent flame regions. When a mushroom flame cap is observed, it forms here.

(3) The non luminous flame of methanol does not have the upper high radiance zone because combustion of soot will not occur near the boundary of the continuous and intermittent flame regions.

(4) The contours of standard deviation give us information about the flame edge and the vortex regions where mushroom flame cap is formed.

(5) The contours of the coefficient of variation identify the limits of the stable flame region.

ACKNOWLEDGMENTS The authors wish to thank Nippon Avionics Co., LTD. for their help with the instrumentation and Dr. Jonh A. Rockett for editorial assistance.

REFERENCES

1. Brötz, W., Schonbucher, A., Scheller, V. and Kettler A, *Combustion and Flame*, Vol.37, pp.1-24, 1980.

2. Hayasaka, H., Koseki, H., and Tashiro, Y., *Fire Technology*, Vol.28(2), pp.110-122, 1992.

3. Hayasaka, H., Koseki, H., and Tashiro, Y., *HTD-Vol. 203, ASME*, pp.71-77, 1992.

4. Thomas, P.H., *Combustion and Flame*, Vol.5, pp.359-367, 1961.

5. McCaffrey, B. J., *Fire Technology*, Vol.24(1), pp.33-47, 1979.

6. Bouhafid, A., Vantelon, J.P., Joulain, P. and Fernandez-Pello, A.C., *Twenty-Second Symp. (Inter.) on Combustion*, The combustion Institute, Pittsburgh, pp.1291-1298, 1988.

7. Ito, A. and Ohata, K., *Thirty-second National (Japanese) Symp. on Combustion*, The combustion Institute of Japan, pp.603-605, 1994.

Discussion

John Rockett: The nominal heat that you used in defining the boundaries between the regions, was that a total nominal heat based on the heat of combustion or did you correct for the radiated fraction so that the heat that you used was the convective heat? The quantity q(C), you said that was a nominal heat of combustion but have you subtracted the radiated fraction so that's the conductive heat or is that the total heat of combustion? Would the boundaries shift to be more similar to the methanol if you corrected for just using the convective heat to normalize the heights?

Hiroshi Hayasaka: That's the total.

Takashi Kashiwagi: In doing the temperature calculation, do you assume asymmetric or symmetric because your temperature distribution showing is not necessary asymmetric although you are looking at only one slice.

Hiroshi Hayasaka: All the figures I showed you, they are not symmetric.

Takashi Kashiwagi: Then how do you get the temperature?

Hiroshi Hayasaka: The temperature distribution was measured using a thermocouple. And as for radiance distribution, a calculation was made based upon thermographic data.